Desalination and Water Treatment
www.deswater.com
doi: 10.5004/dwt.2022.28733

269 (2022) 295–302
September

Stability control of automotive hydraulic system based on ABS coordinated control

Jianwei Liang[a], Aibing Wang[b,*], Baoqiu Ma[a], Jingli Li[c]

[a]*Department of Mechanical and Electrical Engineering, Shijiazhuang University of Applied Technology, Shijiazhuang 050081, China*
[b]*Automotive Engineering Department, Hebei Jiaotong Vocational and Technical College, Shijiazhuang 050035, China, email: uihfsdiojf@163.com*
[c]*Railway Vehicle Department, Hebei Vocational College of Rail Transportation, Shijiazhuang 050022, China*

Received 11 June 2021; Accepted 18 July 2022

ABSTRACT

As an active safety technology, vehicle stability control system can suppress the tendency of excessive steering and serious understeer, and improve the handling stability of vehicles. Equipped with ABS By monitoring the wheel slip state, adjusting the braking pressure of the wheel timely, the wheel speed and speed information are converted into electrical signals, which are sent to the ABS controller to calculate the tire longitudinal slip rate. An upper controller is established to determine the wheel cylinder pressure according to the actual wheel slip rate and the expected slip rate the expected value of force. It can realize the basic pressurization and decompression test, and reach the set value in a short time, meet the requirements of the system. The wheel cylinder pressure is in good agreement with the hardware in the loop test results, that is, the established braking model has good accuracy, which ensures the recovery of braking energy and prevents the wheel from locking.

Keywords: ABS coordinated control; Automobile hydraulic braking; Stability control

1. Introduction

The green intelligent vehicle requires that the braking system reduce or cancel the dependence on the engine vacuum, and the braking feeling is not affected by the coordinated control process of regenerative braking and friction braking, and the braking system can realize low-noise active conventional braking [1]. Automobile braking refers to the ability to stop in a short distance and maintain the stability of driving direction, as well as the ability to maintain a certain speed in uphill and downhill. The braking performance of automobile is one of the main performances of automobile, which is directly related to traffic safety [2]. For the automotive electro-hydraulic brake system, it uses electronic components to replace part of the mechanical components of the traditional hydraulic braking system, which is a hybrid system of mechanical, electrical and hydraulic. Therefore, the system has strong nonlinear characteristics, including the compressibility of the brake fluid, the hysteresis effect of the brake pipeline, the damping effect of the solenoid valve, etc., it is very difficult to control the brake wheel cylinder pressure quickly [3].

The main causes of vehicle instability are as follows: (1) Oversteering is caused under certain driving conditions, such as the transfer of axle load caused by vehicle longitudinal and lateral acceleration. In some cases, the vehicle can be changed from understeer to oversteer, thus leading to vehicle instability. (2) Because of the longitudinal force

* Corresponding author.

produced by the braking or driving of the tire, the cornering stiffness of the tire will be reduced, which will cause the side slip of the front or rear axle and cause instability [4]. (3) The yaw rate produced by the vehicle often lags behind the driver's control of the steering wheel. When the vehicle changes lanes in an emergency, the vehicle will produce a relatively large yaw moment when steering, which will cause a large side slip angle of the vehicle's center of mass after a period of time. It is difficult for the driver to control the vehicle under a large side slip angle of the mass center, which leads to instability.

In order to adjust the brake wheel cylinder pressure accurately, many control strategies have been applied to the control of automobile brake system [5]. Among them, logic gate limit control, PID, fuzzy control and neural network control have been applied in automobile braking system, and achieved certain control effect. However, because they are not model-based control methods, some characteristics of the brake system are ignored in the design of the control strategy, and it is difficult to accurately monitor the state of the brake system [6].

In this paper, the stability control of automotive hydraulic braking system based on ABS coordinated control is studied by monitoring the wheel slip state, adjusting the braking pressure of the wheel timely, the wheel speed and speed information are converted into electrical signals, which are sent to the ABS controller to calculate the tire longitudinal slip rate. An upper controller is established to determine the wheel cylinder pressure according to the actual wheel slip rate and the expected slip rate the expected value of force [7].

2. ABS coordinated control

Active safety system is an anti-lock brake system (ABS). It uses the relationship between the road and the tire system to control the wheel slip rate at the critical point, so as to give full play to the road adhesion performance and achieve the best effect [8]. It can effectively prevent side slip, tail flick and loss of steering ability caused by locking.

ABS automobile anti-lock system mainly includes speed sensor, wheel speed sensor, main control unit, hydraulic adjustment unit, conventional hydraulic braking system and alarm system, etc. its specific structure is shown in Fig. 1.

The wheel speed sensor is installed on the wheel of the car, and the speed sensor is also installed on the car body to convert the wheel speed and speed information into electrical signals and send them to the ABS controller. After calculation, the slip rate is obtained, and the corresponding control signal of the high-speed on-off valve is output according to the slip rate [9]. When the actual slip rate is less than 20%, the ABS controller makes the normally open high-speed on-off valve 5 open and the normally closed high-speed on-off valve 4 close to realize the pressurization of the hydraulic system; when the slip ratio is equal to 20%, the ABS controller closes the normally open high-speed switch valve 5 and the normally closed high-speed on-off valve 4 to maintain the pressure of the hydraulic system; When the slip ratio is more than 20%, the ABS controller makes the normally open high-speed on-off valve 5 close and the normally closed high-speed on-off valve 4 open to realize the system pressure reduction. In addition, in order to monitor the various parts of ABS, the electronic control unit is also equipped with a monitoring device. Once these components have abnormal conditions, it will trigger the alarm device to give an alarm, and exit the ABS brake and turn to the hydraulic conventional braking.

ABS controller model is a simplified ABS control model [10]. The modeling of this module is to adjust the braking torque of each wheel by controlling the hydraulic adjusting unit. The ABS controller module is specially used for four-wheel vehicles. If one or more wheels are detected to be about to lock up under braking conditions, the ABS controller model will provide appropriate torque adjustment to avoid wheel locking [11]. This simplified method is to calculate the approximate value of tire longitudinal slip ratio (using wheel rotation speed and vehicle speed as input and tire rolling radius as parameter).

(1) ABS full supervision stage: if the estimated tire longitudinal slip rate is lower than $S_{x\mathrm{ABS}}(1 + x)$, the controller model will release the input braking torque completely until it drops to zero. The output ABS supervision braking torque of each wheel is:

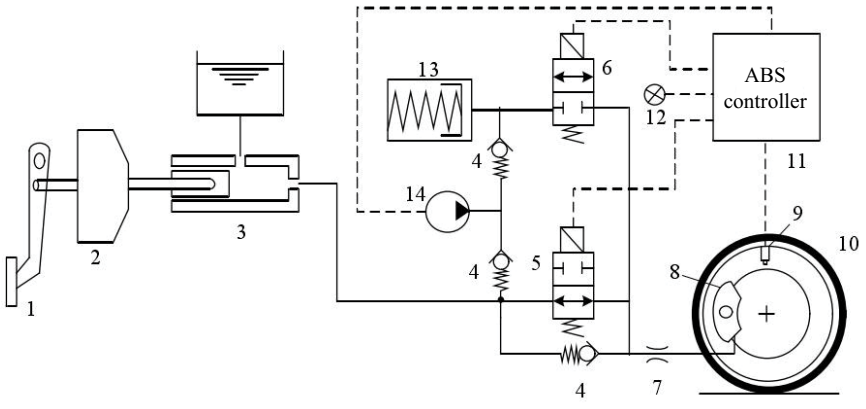

Fig. 1. Structure of ABS hydraulic system.

$$T_{\text{brake}} = 0 \tag{1}$$

(2) ABS partial supervision stage: if the estimated tire longitudinal slip rate is within the specified boundary area $S_{x\text{ABS}}(1 + x)$, $S_{x\text{ABS}}(1 - x)$, then the controller model will release the input braking torque using a simple linear function about S_x. The output ABS regulatory braking torque of each wheel is:

$$T_{\text{brake}} = f\left(S_x\right) = \frac{T_{\text{in}}}{2x}\left[-\frac{S_x}{S_{x\text{ABS}}} + 1 + x\right] \tag{2}$$

(3) In the unsupervised phase of ABS: the estimated tire longitudinal slip ratio is in the $[S_{x\text{ABS}}(1 - x), S_{x\text{ASR}}]$ range, and the input braking torque is applied:

$$T_{\text{brake}} = T_{\text{in}} T_{\text{brake}} \tag{3}$$

In Fig. 2 S_x represents the longitudinal slip rate of tire, $S_{x\text{ABS}}$ represents the regulatory value of longitudinal slip rate, x represents the monitoring area of ABS status, F_x represents the tire longitudinal force based on the tire longitudinal slip rate, T_{brakeABS} represents the supervised braking torque, and T_{in} represents the input target torque.

For automobile ABS, the wheel slip rate is generally controlled [12,13]. Therefore, it is necessary to establish an upper controller to determine the expected value of the wheel cylinder pressure according to the actual and expected slip rate of the wheel. The upper controller is designed by sliding mode variable structure control principle. Firstly, the single wheel model is selected as follows:

$$\begin{cases} m\dot{v} = -F_x \\ I_w\dot{\omega} = rF_x - T_b \end{cases} \tag{4}$$

where m is the mass of the vehicle, $\dot{v}$ is the longitudinal speed of the vehicle, F_x is the longitudinal force of the tire, I_w is the rotational inertia of the wheel, $\dot{\omega}$ is the angular velocity of the wheel, r is the effective rolling radius of the tire, and T_b is the braking torque.

The difference between the actual value s and the expected value s_d and its derivative are selected as the state variables of the sliding mode switching function:

$$\begin{cases} e = s - s_d \\ \dot{e} = \dot{s} \end{cases} \tag{5}$$

If c is a constant, then the sliding mode switching function is:

$$\delta = c_e + \dot{e} = \dot{s} + c\left(s - s_d\right) \tag{6}$$

The sliding mode control term is the combination of constant velocity reaching rate and continuous function as follows:

$$\dot{\delta} = c\dot{e} + \dot{e} = -\varepsilon\tanh\left(\delta/\Omega\right) \tag{7}$$

where ε is the constant velocity approach law, and its value greater than 0, Ω is the saturation interval parameter of the continuous function tanh. Due to the inertia effect of the electro-hydraulic braking system, the following equation is used to describe the lag of braking torque:

$$\dot{T}_b = \frac{U_{\text{Tb}} - T_b}{T_h} \tag{8}$$

where U_{Tb} is the output control value of the braking torque based on sliding mode control and T_h is the time constant of the first-order inertial link. The output braking torque control value U_{Tb} of sliding mode controller is obtained as follows:

$$U_{\text{Tb}} = I_w T_h\left\{\varepsilon\tanh\left(\delta/\Omega\right) + \left(c - \frac{2\dot{v}}{v}\right) + \frac{1}{I_w T_h}\left(-I_w\dot{\omega} + F_x r\right)\right\} \tag{9}$$

The ABS pavement conditions are set as butt flat pavement, and the pavement adhesion coefficient and expected slip ratio are shown in Table 1. The test condition is that the

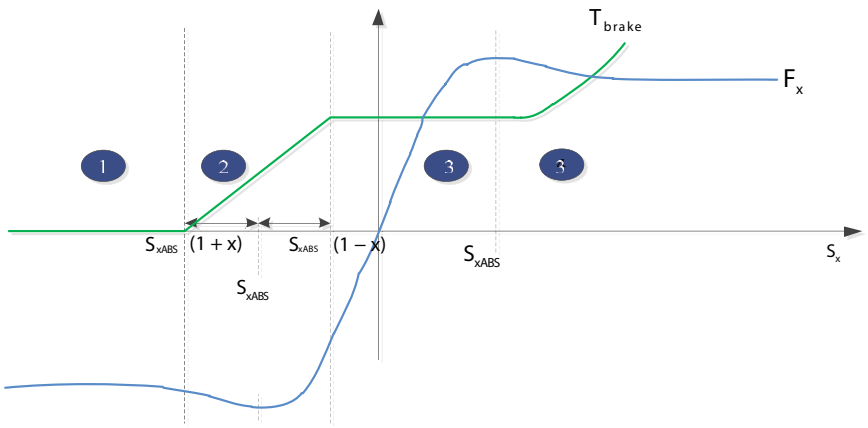

Fig. 2. ABS controller module status monitoring diagram.

Table 1
Road adhesion coefficient and expected slip ratio

Braking distance	<50 m	50–100 m	>100 m
Road adhesion coefficient	0.5	0.2	0.8
Expected slip ratio	0.117	0.08	0.15

vehicle makes emergency braking on the road at the initial speed of 120 km/h.

3. Stability control of automobile hydraulic braking system

When the vehicle is running, it is affected by the road conditions. When the adhesion reaches the adhesion limit, the dynamic performance of the vehicle will change [14]. The adhesion includes longitudinal force and lateral force. When the longitudinal force reaches the adhesion limit, it will affect the driving performance or braking performance of the vehicle. Similarly, when the lateral force reaches the adhesion limit, it will affect the lateral performance of the vehicle and the dynamic stability performance of the vehicle.

The judgment of wheel stability is mainly to judge whether the wheel is in the locking state, and the vehicle stability is mainly to judge whether the vehicle yaw rate and the side slip angle of the vehicle center are within the stable range of the vehicle, so as to judge whether the vehicle is in the stable state [15]. The importance of motor as an electric vehicle has been mentioned before, but this system mainly uses the reversibility of Brushless DC motor, so the maximum braking torque of motor has a great impact on the recovery of braking energy. The torque output characteristics of the motor in this paper can be simulated by the first-order inertia delay mathematical model, and the torque output can be expressed as follows:

$$T_m = \frac{1}{1 + t_r s} T_{\min} \tag{10}$$

where T_m is the actual torque (nm), t_r is the time constant (s), and $T_{\min}$ is the maximum torque of the motor.

The electric energy of the motor in the generating state is converted from the mechanical inertia energy, and the energy is expressed as follows:

$$P_{\text{el}} = P_{\text{mec}} + P_{\text{lost}} \tag{11}$$

where P_{el} is the generating power (W) of the motor, P_{mec} is the driving power (W) of the motor, and P_{lost} is the power lost during the conversion (W).

With the hardware of ABS and TCS system, better control effect can be obtained with less modification. When the sideslip angle of vehicle center of mass is close to zero, the yaw rate reflects the turning ability of the car. The higher the yaw rate of the car is, the stronger the turning is, the smaller the turning radius is, and vice versa [16,17]. Therefore, when the side slip angle of the vehicle center is small, the yaw rate represents the running track of the vehicle.

When the side slip angle of the vehicle is very small, the yaw rate determined by the linear two degree of freedom vehicle is the most stable for the vehicle. Fig. 3 shows the steering characteristics of a linear two degree of freedom vehicle. The forward speed of the vehicle is V_x, the side slip angle of the center of mass is β, the front wheel angle is δ, the distance from the center to the front and rear axle is a and b respectively, the yaw rate of the vehicle is γ, the equivalent lateral stiffness of the front and rear axles is K_f and K_r, and the rotational inertia of the vehicle around the z-axis is I_z.

The steady-state steering characteristics of linear 2-DOF vehicle are selected as the ideal representation of yaw rate and sideslip angle of mass center on vehicle stability [18].

$$\begin{cases} r_{\text{NO}} = G_\gamma \cdot \delta \\ \beta_{\text{NO}} = G_\beta \cdot \delta \end{cases} \tag{12}$$

where G_γ is the steady-state gain of yaw rate and G_β is the steady-state gain of sideslip angle. The limit conditions for the lateral adhesion of the tire must be as follows:

$$\left|a_y\right| \le \mu \cdot g \tag{13}$$

When the steering wheel is turned, the ground has a lateral force on the wheel, which produces a yaw moment on the car, which further changes the yaw rate of the car. However, the yaw moment also depends on the side slip angle of the vehicle. With the increase of yaw angle, the gain of yaw moment decreases. At large yaw angle, when the steering wheel angle changes, the yaw moment almost does not change. Especially in the physical limit, the car lost the steerability. On dry asphalt pavement, the deflection angle of the physical limit is 12, while on ice pavement, the limit value is 2. If the side slip angle of the vehicle reaches the characteristic value, the car will lose control and cause traffic accidents. Therefore, the sideslip angle should be limited to the eigenvalue β_T.

Because it is difficult to determine the quasi stable state tolerance of the yaw angle, and when only using the scalar feedback control of yaw rate state, the control effect is not ideal because of too large sideslip angle, so the stability range of side slip angle is expressed by the following inequality:

$$\left|\beta + B_1\dot{\beta}\right| \le B_2 \tag{14}$$

where B_1 and B_2 are constants. The inequality is derived from the test results shown in Fig. 4. When the inequality is established, the driving state of the vehicle is considered to be stable, otherwise, it is considered that the vehicle will lose its dynamic stability.

The quasi stable tolerance of yaw rate can be determined as follows:

$$\left|\Delta\gamma\right| \le \left|c\gamma_{\text{NO}}\right| \tag{15}$$

If the inequality is true, the vehicle is considered to be stable; if not, it is considered that the vehicle loses stability and needs to be controlled. Therefore, after the quasi

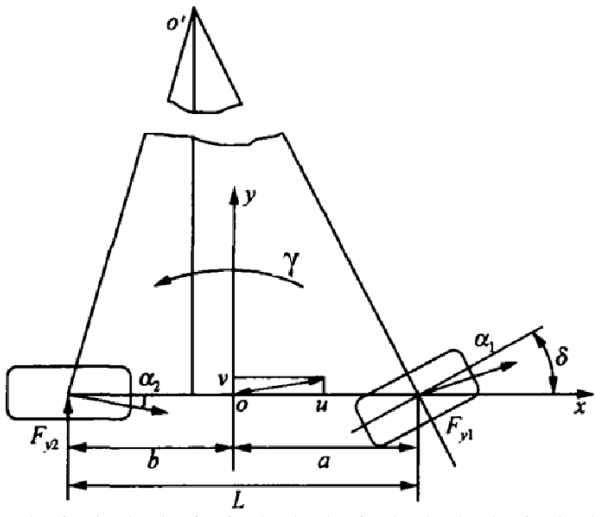

Fig. 3. Linear two degree of freedom vehicle model.

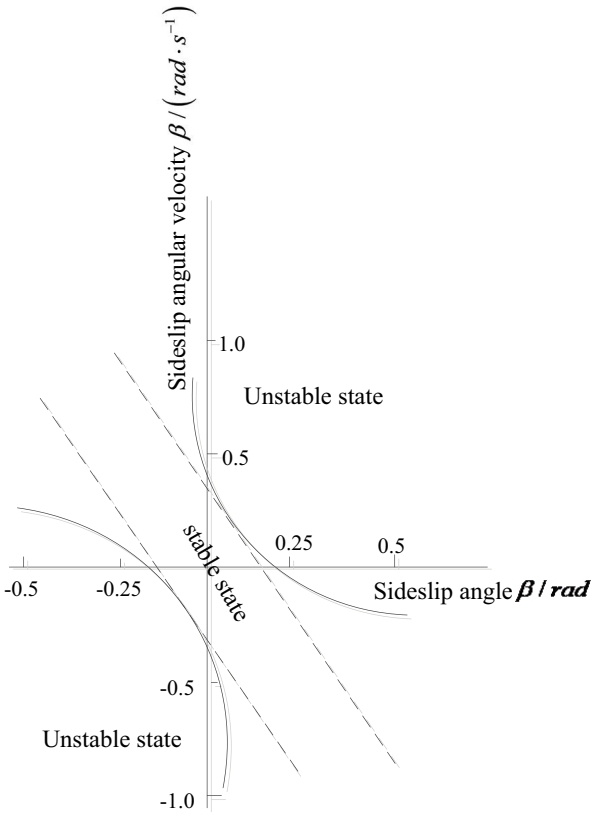

Fig. 4. Stability criterion of side slip angle.

stable tolerance zone of yaw rate and sideslip angle of mass center is determined, the driving stability of vehicle can be judged. As long as one of the driving states does not conform to the above two inequalities, the vehicle is controlled so that the yaw rate and sideslip angle are within the stable tolerance zone [19].

Wheel stability can be expressed by wheel slip ratio. When the wheel slip ratio reaches a critical point, even if the braking pressure of the wheel remains unchanged, the wheel slip rate will continue to increase, which is the boundary point between the stability and instability of the wheel. The critical point of the slip rate changes with the change of the road adhesion coefficient [20,21].

From Fig. 5 there are two stable boundaries in the graph: one is the basic boundary, and the other is the actual boundary obtained after correction. The basic boundary is determined by wheel slip rate and wheel deceleration. In order to reduce the false triggering of ABS, the basic boundary is modified. The modified threshold value of slip ratio can be expressed as follows:

$$S_{w-th} = f\left(a_w\right) + S_{\text{off}} \tag{16}$$

$$S_{\text{off}} = S_a + S_{\mu} + S_{s'} + S_{\text{si}} \tag{17}$$

where $S_{w\text{–th}}$ is the threshold value of wheel slip stability, S_{off} is the correction of threshold value of wheel slip rate, S_a is the correction of threshold value of slip rate determined by the range of wheel deceleration, S_{μ} is the correction amount of threshold value of slip rate determined by road adhesion state, $S_{s'}$ is the correction amount of threshold value of slip rate determined by wheel slip speed, and S_{si} is determined by integral value of wheel slip rate. The modified value of sliding rate threshold value is fixed.

The correction of the threshold value of wheel slip rate is wheel slip rate speed, wheel slip integral value, wheel adhesion coefficient and wheel deceleration. When the speed of wheel slip rate is small, reduce the threshold value correction of car wheel slip rate to improve the sensitivity of ABS intervention to prevent wheel lock during slow braking; when the integral value of wheel slip rate is large in a certain period of time, it shows that the wheel tends to be unstable gradually, so reduce the threshold correction of slip rate to improve the sensitivity of ABS control; When the road adhesion is rough, increase the threshold correction of slip rate to reduce the sensitivity of ABS control. When the road adhesion is separated, the correction of slip rate threshold is reduced to improve the road surface Sensitivity of ABS control; when the deceleration of wheels is within the deceleration range of typical ice and snow pavement and no vehicle is detected on rough road or separated road, increase the correction value of slip rate threshold to reduce the sensitivity of ABS on ice and snow pavement, and prevent the wrong triggering of ABS on ice and snow pavement [22].

4. Experimental study

In this experiment, through the experiment of sharp turning and emergency avoidance on the rainy road and dry road, through the extraction and analysis of the experimental results, to verify the rationality and effectiveness of predictive control for vehicle stability control. The real-time platform of hardware in the loop test-bed adopts micro auto box and rapid Pro rapid control prototype system, relay, upper computer, MATLAB/Simulink and control desk produced by D space company The system is used to test and control the electro-hydraulic brake system, collect and

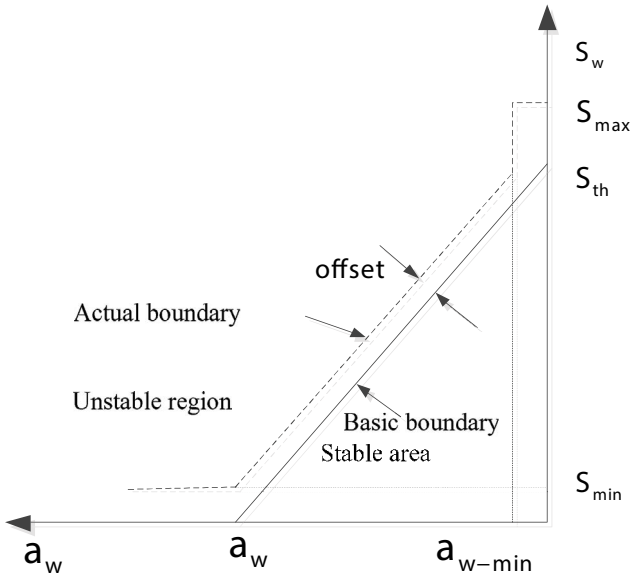

Fig. 5. Wheel stability boundary.

Fig. 6. Physical diagram of system test bench.

process various sensor information in real time, calculate the vehicle dynamic model, and drive the motor, solenoid valve and other components in the hydraulic control unit. Physical diagram of system test bench is shown in Fig. 6.

The master cylinder, pedal feeling simulator and hydraulic control unit of the electro-hydraulic braking system are shown in Fig. 7.

The solenoid valve mentioned in the hydraulic control unit is mainly for the high-speed on-off valve, and its parameter setting is shown in Table 2.

The test bench, control unit and control strategy of the electro-hydraulic braking system are applied to carry out the basic brake pressure increasing and reducing pressure test. The test results are shown in Fig. 8.

Set the reference pressure signal to 6 MPa for test, the results show that the system can rise to the set value in 100 ms and keep stable; the system can reduce the wheel cylinder pressure from 6 MPa to 0 within 70 ms. It can be seen from Fig. 8 that the system can realize the

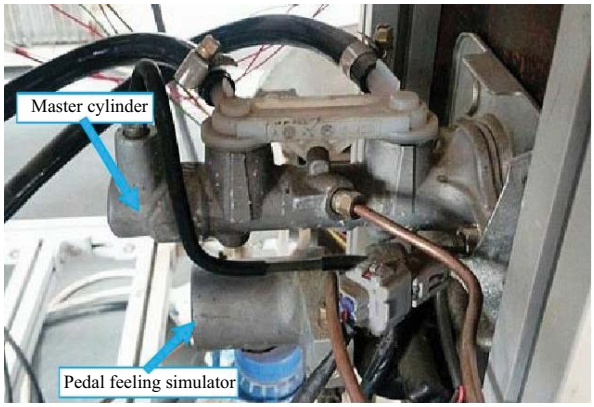

(a)

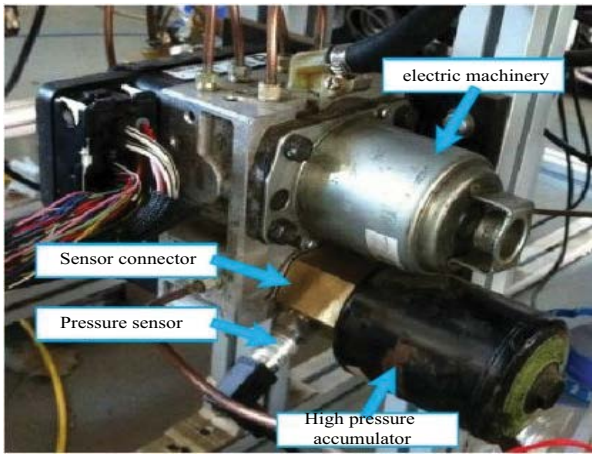

(b)

Fig. 7. (a) Master cylinder and pedal feeling simulator and (b) hydraulic control unit.

basic pressurization and decompression test, and reach the set value in a short time, meeting the requirements of the system. It shows that the test bench and control strategy meet the test requirements and can be used for test verification of complex signals [23].

The hardware in the loop test results and simulation results of wheel cylinder pressure under the same conditions are shown in Fig. 9.

It can be seen from Fig. 9 that under the same conditions, the wheel cylinder pressure obtained from the simulation test is in good agreement with the hardware in the loop test results, that is, the brake model established has good accuracy, and it also shows that the model parameter values identified by ABS coordinated control have strong credibility.

From Fig. 10, when the wheel slip ratio reaches a critical point, even if the wheel braking pressure remains unchanged, the wheel slip rate will continue to increase, which is the boundary point between wheel stability and instability. When braking on low adhesion coefficient road, with the increase of master cylinder brake pressure, ABS will be triggered ABS control can be well coordinated to

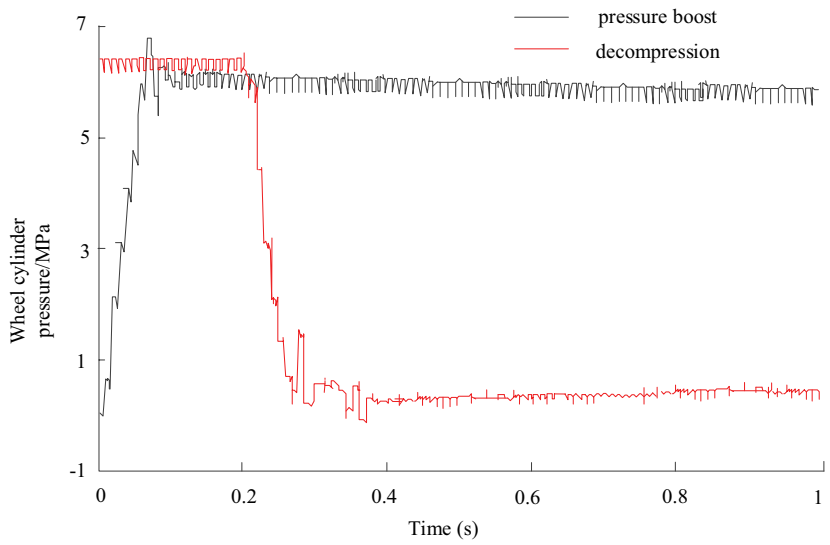

Fig. 8. Test results of system basic brake pressurization and decompression.

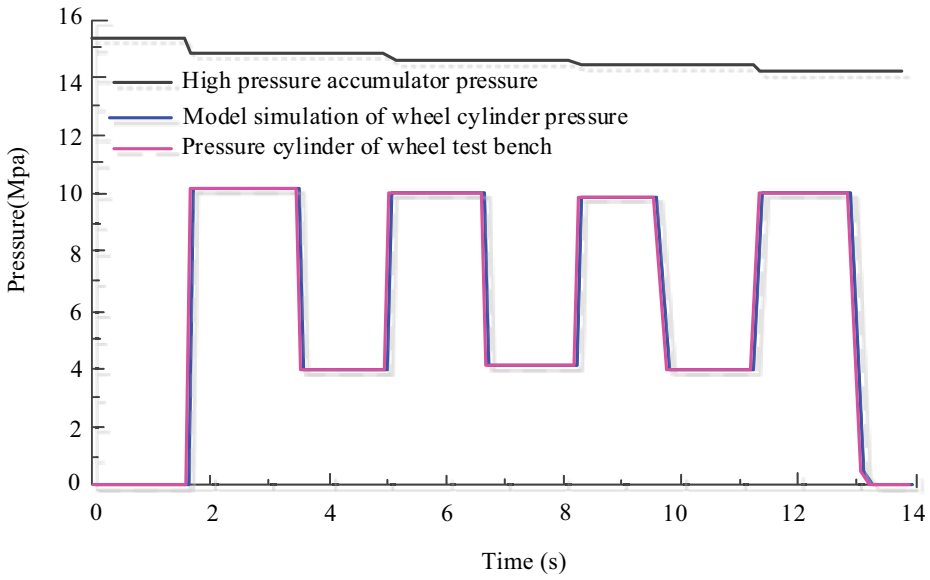

Fig. 9. Wheel cylinder pressure of hardware in the loop test and simulation test.

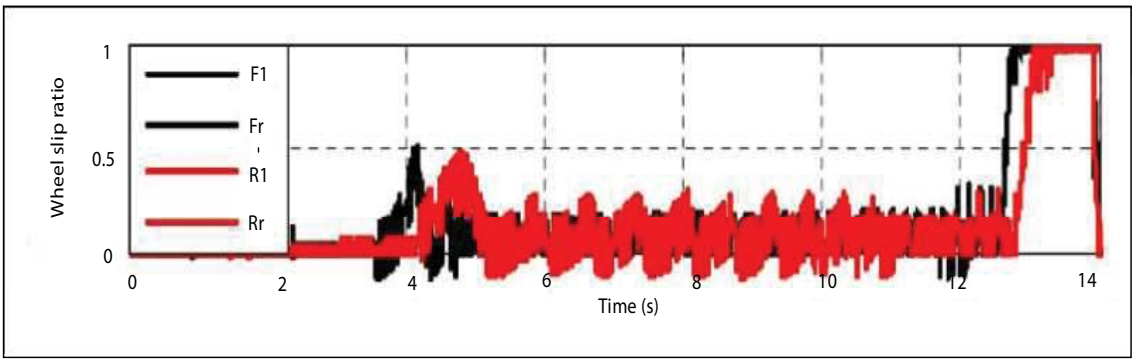

Fig. 10. Time history curve of wheel slip rate.

Table 2
Parameter setting of hydraulic regulating unit module

Parameter name	Numerical value
Maximum flow coefficient	0.7
Reynolds number	100
Orifice diameter	0.6 mm
Area at maximum opening of solenoid valve	0.4 mm^2

ensure the recovery of braking energy and prevent wheel locking.

5. Conclusion

This paper analyzes the working principle of traditional hydraulic braking and motor regenerative braking with ABS anti-lock function. Based on the structure of pure electric vehicle power steering system studied in this paper, a compound braking system which can realize vehicle conventional braking, anti-lock braking and energy recovery is designed. In fact, the pressure in the high-pressure accumulator is constantly changing when the electro-hydraulic braking system is working. The next step is to establish the model of motor pump and high-pressure accumulator, and to study their influence on wheel cylinder pressure. In addition, the flow rate of the brake system can also be introduced into the verification of the system model.

References

[1] W. Han, L. Xiong, Z.P. Yu, Braking pressure control in electro-hydraulic brake system based on pressure estimation with nonlinearities and uncertainties, Mech. Syst. Sig. Process., 131 (2019) 703–727.
[2] Y. Yang, Y.D. He, Z. Yang, C.Y. Fu, Z.P. Cong, Torque coordination control of an electro-hydraulic composite brake system during mode switching based on braking intention, Energies, 13 (2020) 2031, doi: 10.3390/en13082031.
[3] J. Zhao, D.J. Song, B. Zhu, Z.C. Chen, Y.H. Sun, Nonlinear backstepping control of electro-hydraulic brake system based on bond graph model, IEEE Access, 8 (2020) 19100–19112.
[4] Q.P. Chen, H.Y. Sun, N. Wang, Z. Niu, R. Wan Sliding mode control of hydraulic pressure in electro-hydraulic brake system based on the linearization of higher-order model, Fluid Dyn. Mater. Process., 16 (2020) 513–524.
[5] Y. Yuan, J.Z. Zhang, Y.T. Li, C. Li, A novel regenerative electrohydraulic brake system: development and hardware-in-loop tests, IEEE Trans. Veh. Technol., 67 (2018) 11440–11452.
[6] P. Kachanov, O. Lytviak, O. Derevyanko, S. Komar, Development of an automated hydraulic brake control system for testing aircraft turboshaft gas turbine engines, Eastern-European J. Enterp. Technol., 6 (2019) 52–57.
[7] C. Feng, Key technologies of low carbon design integrated system for typical automobile parts, J. Comput. Methods Sci. Eng., 19 (2019) S115–S122.
[8] S. Cheng, L. Li, H.-Q. Guo, Z.-G. Chen, P. Song, Longitudinal collision avoidance and lateral stability adaptive control system based on MPC of autonomous vehicles, IEEE Trans. Intell. Transp. Syst., 21 (2020) 2376–2385.
[9] Z. Chen, J. Wu, J. Zhao, R. He, S. Qi, Control strategy for accurate adjustment of braking force in hybrid brake by wire system, Qiche Gongcheng/Autom. Eng., 40 (2018) 457–464.
[10] X.-h. Zeng, G.-h. Li, D.-f. Song, S. Li, Z.-c. Zhu, Active anti-rollover control for hydraulic hub-motor hybrid system of heavy commercial vehicle, J. Jilin Univ. (Eng. Technol. Ed.), 48 (2018) 1–10, doi: 10.13229/j.cnki.jdxbgxb20161398.
[11] Z.X. He, Y.B. Feng, Y. Liu, L. Li, C.L. Ma, H. Wang, Semi-physical real-time control of electro-hydraulic proportional position servo system based on Matlab/xPC, J. Eng., 2019 (2019) 144–149.
[12] R. Iskovich-Lototsky, Terms of the stability for the control valve of the hydraulic impulse drive of vibrating and vibro-impact machines, Przeglad Elektrotechniczny, 1 (2019) 21–25.
[13] J. Li, F. Wang, Y. He, Electric vehicle routing problem with battery swapping considering energy consumption and carbon emissions, Sustainability (Basel, Switzerland), 12 (2020) 10537, doi: 10.3390/su122410537.
[14] Y. Zhu, S. Tang, C. Wang, W.L. Jiang, J.H. Zhao, G.P. Li, Absolute stability condition derivation for position closed-loop system in hydraulic automatic gauge control, Processes, 7 (2019) 1–16.
[15] K. Gong, C.C. Song, J.H. Bu, C. Ma, Research on industrial control technology of hydraulic stability of condensing unit on ethanol distillation tower, J. Phys. Conf. Ser., 1550 (2020) 062016.
[16] X.Y. Peng, K.H. Wen, Control strategy of optimal braking force distribution for vehicle with brake-by-wire system after single wheel brake failure, J. Hunan Univ. Nat. Sci., 45 (2018) 44–53.
[17] C.Z. Luo, F. Zhang, Analysis on hydraulic stability of large pumped storage unit and corresponding precontrol measures, Mechanical and Electrical Technique of Hydropower Station, 41 (2018) 1–5, 15.
[18] J.Y. Lv, H.L. Zhang, M.J. Liu, Application research of CAN bus in automobile detection technology, J. Comput. Methods Sci. Eng., 19 (2019) S123–S130.
[19] X.Y. Niu, G.S. Feng, Torque distribution control of hybrid electric bus with composite power supply based on particle swarm optimization, J. Comput. Methods Sci. Eng., 20 (2020) 365–381.
[20] K. Zhang, Md Halim Shalehy, G. Tawfiq Ezaz, A. Chakraborty, K. Mushfique Mohib, L.X. Liu, An integrated flood risk assessment approach based on coupled hydrological-hydraulic modeling and bottom-up hazard vulnerability analysis, Environ. Modell. Software, 148 (2022) 105279, doi: 10.1016/j.envsoft.2021.105279.
[21] B. Wang, L.M. Zhang, H.R. Ma, H.X. Wang, S. Wan, Parallel LSTM-based regional integrated energy system multienergy source-load information interactive energy prediction, Complexity (New York, N.Y.), 2019 (2019) 1–13.
[22] Y.F. Zha, G.Q. Liu, F.W. Ma, R.H. Guo, Acceleration slip regulation control for four-wheel independently drive electric vehicle based on fuzzy control, J. Comput. Methods Sci. Eng., 20 (2020) 1265–1278.
[23] Q.Y. Zhang, Z.F. Lu, Y.R. Wang, W.P. Lin, Driving pattern recognition of hybrid electric vehicles based on multi-hierarchical fuzzy comprehensive evaluation, Jordan J. Mech. Ind. Eng., 14 (2020) 159–165.